IEEE Access
Multidisciplinary | Rapid Review | Open Access Journal

Received April 17, 2020, accepted May 5, 2020, date of publication May 22, 2020, date of current version June 25, 2020.

Digital Object Identifier 10.1109/ACCESS.2020.2996707

W-Band Low Phase Sensitivity Reflectarray Antennas With Wideband Characteristics Considering the Effect of Angle of Incidence

EUN-CHEOL CHOI AND SANGWOOK NAM, (Senior Member, IEEE)
School of Electrical and Computer Engineering, Institute of New Media Communication, Seoul National University, Seoul 08826, South Korea
Corresponding author: Sangwook Nam (snam@snu.ac.kr)

This work was supported in part by the Center for Advanced Meta-Material funded by the Ministry of Science, ICT, and in part by the Future Planning as Global Frontier Project under Grant CAMM-2014M3A6B3063708.

ABSTRACT In this study, a W-band reflectarray antenna is designed with the characteristics of low phase sensitivity and wideband. Low phase sensitivity is achieved by subdividing the unit cell variation method into five steps. While designing a unit cell with low phase sensitivity, phase distortion may occur within the target bandwidth with varying incident angles of illumination, resulting in a limited bandwidth. The origin of large-phase distortion is analyzed based on the input impedance of multiresonant elements, considering the incident angle. This study suggests a selection strategy of the variation steps in the reflectarray by using the relative phase requirement based on the structural dimensions of the proposed antenna. An offset feed reflectarray with $12\lambda_0$ aperture diameter at 90 GHz center frequency is designed using the proposed method. The measured gain is 28.5 dBi at 90 GHz, and the maximum efficiency is 55.3% at 82 GHz. The measured 1-dB gain bandwidth is approximately 28.8% in the W-band of 81−107 GHz.

INDEX TERMS Angle of incidence, low phase sensitivity, millimeter wave, reflectarray antenna, wideband.

I. INTRODUCTION

A microstrip reflectarray antenna is a combination of a reflector antenna and phased-array antenna, in which a curved conductor reflector antenna is converted into a planar array antenna with appropriate phase compensation of the radiating element [1]. Compared to the curved conductor reflector antenna, the microstrip reflectarray has advantages such as high efficiency, low cost, low profile, easy fabrication, and reconfiguration [2], [3]. Presently, high-gain reflectarray antennas are widely used in applications such as millimeter wave radars, remote sensing, and target detection [4], [5]. Millimeter-wave sensors are suited to many radar systems, because the wavelength is short enough to obtain high spatial resolution. Furthermore, these frequencies permit large bandwidths and improve system performance [6]. However, there are two critical problems in designing a wideband reflectarray antenna at millimeter-waves. The first problem is the phase sensitivity according to the variation of element length. If the unit cell is designed by only considering the target performance and not the fabrication accuracy, the desired performance may not be achieved [7]–[9]. In the case of a millimeter-wave reflectarray, the phase resolution should be set considering the fabrication tolerance. If the phase sensitivity is high according to the variation of the element length, the performance of the antenna may degrade because of manufacturing issues. Therefore, the antenna must be designed such that the phase sensitivity decreases as the frequency increases. However, as the unit cell is composed of a resonant element, the reflection phase shows an S-curve characteristic, where the phase rapidly changes near the resonance. Therefore, various methods have been proposed to prevent the abrupt phase change in the resonance part. In [10], the phase sensitivity was reduced by subdividing the length variation of a single loop into four steps rather than varying the one step in the conventional method [11]. This method improved the maximum sensitivity from 1200°/mm to 200°/mm. In [12], the authors proposed a Phoenix unit cell that changes only one element in the middle, while fixing the inner square patch and outer square loop element. The total phase range could be easily widened to 360° owing to the use of multiple resonant elements and variation in only one middle element, and the

The associate editor coordinating the review of this manuscript and approving it for publication was Mohammad Tariqul Islam.

phase sensitivity was significantly reduced to 148°/mm compared to that using the conventional method of multiresonant elements [13]. The two aforementioned methods [10], [12] allowed more diverse variation than that allowed by the conventional methods. However, as these methods change only one element, the steps that can be subdivided to lower the sensitivity are limited, and hence the phase sensitivity is still considered to be higher. Moreover, the phase sensitivity required for a W-band or a higher band is much lower than the values achieved by these methods.

The second problem is the reduction of the gain bandwidth due to the inherent narrowband characteristics of the unit cell. In general, the bandwidth of the elements is 3–5%, indicating that broadband characteristics cannot be obtained in the usual manner. To address this problem, various techniques, such as the use of a stack of unit cells, sub-wavelength periodicity, and multi-resonance unit cells, have been proposed [14]–[18]. However, although a wide phase range can be obtained by using a stack of unit cell, a stack is difficult to manufacture and is expensive. For sub-wavelength periodicity, it is difficult to obtain a phase range of 360° because of reduced periodicity. Further, in the case of multiresonant elements, the conventional method of simultaneously varying all the elements can easily obtain a wide phase range; however, the phase sensitivity deteriorates. In addition, when designing a wideband reflectarray, the phase characteristics should be investigated according to the angle of incidence. When the angle of incidence is varied, additional resonance may occur within the target bandwidth, which can result in serious phase distortion. However, to date, this problem has not been rigorously analyzed. Thus, a solution for phase distortion is required considering the angle of incidence to obtain the wideband characteristics.

In this paper, we propose a unit cell with low phase sensitivity and wideband characteristics. The outline of this paper is as follows. Section II describes the design approach for a low phase sensitivity unit cell achieved by individual subdivision of the variation step. Section III presents the analysis of the resonance characteristics and reflection phase of the unit cell considering the incident angle, and describes the arrangement method of elements in a reflectarray surface for the wideband characteristic. In section IV, we discuss about the fabrication and measurement of the prototype of the reflectarray antenna. Finally, the conclusion and summarization of this work are given in section V. All simulations are conducted using full-wave CST Microwave Studio.

II. LOW PHASE SENSITIVITY UNIT CELL DESIGN

Fig. 1 shows the proposed unit cell configuration. The dielectric substrate is Duroid 5880 with relative permittivity $\varepsilon_r = 2.2$, loss tangent $\tan\delta = 0.0009$, and a thickness of 0.254 mm at 10 GHz. To obtain the small total range and low slope of reflection phase, the unit cell with the air gap have been used [12], [19]. The dual-resonant elements of patch and loop configuration are used with an air gap of 0.7 mm. The periodicity of the unit cell is set at

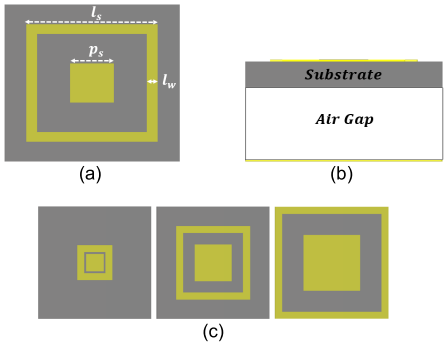

FIGURE 1. (a) Top view and (b) side view of proposed unit cell configuration, (c) Conventional variation method (corresponding to $l_s = 0.5$ mm to 1.6 mm, $p_s = 0.5\ l_s$, and $l_w = 0.1$ mm).

approximately $0.48\lambda_0$ ($f_0 = 90$ GHz) i.e., 1.6 mm to avoid the generation of the grating lobe. A figure of merit for a typical unit cell is the total phase range and phase sensitivity according to dimension variation. Therefore, to cover the compensation phase of the element depending on its position on the array surface, the phase range of 360° must be satisfied, and an appropriate phase sensitivity is required for high efficiency. In general, a unit cell composed of multiresonant elements uses a conventional design method that varies all the elements simultaneously. Fig. 1 (c) shows the conventional variation method, in which the change in the input impedance is large because all the elements are varied simultaneously, such that a large reflection phase shift is observed even with a small variation in the dimensions. As the frequency increases, high phase sensitivity can result in high phase errors depending on the fabrication tolerances. Therefore, in a high frequency band, a low phase sensitivity characteristic is required, considering fabrication accuracy. Low phase sensitivity characteristic can be realized by minimizing the change in the impedance according to dimension variation. Thus, designing a multi-resonance unit cell in the high-frequency band by individually varying the elements and subdividing the variation steps is considered more efficient than the conventional design method of simultaneously varying all elements and using only one step. Fig. 2 shows the unit cell variation step of the proposed variation method and the reflection phase at each step, and Fig. 3 and Table 1 show the comparison between the reflection phase of the conventional and proposed variation methods. The proposed variation method is subdivided into five steps to minimize phase sensitivity. In the first step, a phase range of 9° is derived by varying only the width of the loop and fixing the patch size. In the second step, only the loop size is varied, whereas the patch size is fixed to achieve a phase range of 197° and maximum phase sensitivity of 25°/0.1mm. The subsequent steps are further subdivided into the third and fourth steps to prevent an abrupt phase shift due to the vicinity of unit cell resonance. In the third step, a phase range of 27° and maximum sensitivity of 16°/0.1mm are derived by changing only the patch size while fixing the loop size. In the fourth step, a phase range

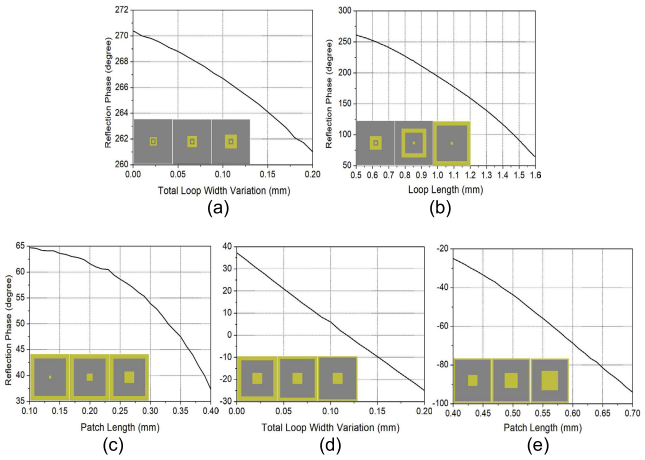

FIGURE 2. Procedure of proposed variation method and reflection phase for normal incidence (a) Step 1 (variation of a total loop width), (b) Step 2 (variation of a loop length), (c) Step 3 (variation of a patch length), (d) Step 4 (variation of a total loop width), (e) Step 5 (variation of a patch length).

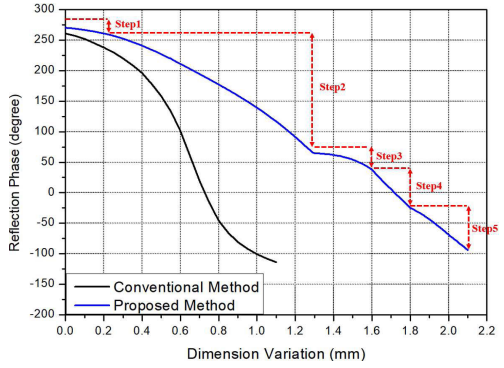

FIGURE 3. Reflection phase of conventional and proposed variation methods for normal incidence at 90 GHz.

TABLE 1. Reflection phase range and its maximum and average sensitivities.

Method	Phase Range (°)	Maximum Sensitivity (°/0.1mm)	Average Sensitivity (°/0.1mm)
Conventional (Total)	375	82	34
Proposed (Total)	364	31	17.3
Step 1	9	5	
Step 2	197	25	
Step 3	27	16	
Step 4	62	31	
Step 5	70	25	

of 62° and maximum sensitivity of 31°/0.1mm are derived by reducing the loop width while fixing the patch size. Finally, in the fifth step, only the size of the patch is varied while the size of the loop is fixed, resulting in a phase range of 70° and maximum phase sensitivity of 25°/0.1 mm. In addition, the total average phase sensitivity should be evaluated along with the maximum sensitivity. If a large number of elements with high sensitivity are placed on the array surface, the total phase error of the aperture increases. Therefore, the average phase sensitivity of all dimensions should be low to reduce the total phase error. The total average phase sensitivity obtained using the proposed method is 17.3°/0.1 mm, which satisfies the aforementioned condition, and the maximum phase sensitivity and average phase sensitivity are significantly improved compared with those obtained using the conventional variation method. Table 2 presents a comparison of recently published performances of unit cells with low phase sensitivity with that of our study. In the previous low phase sensitivity unit cells, the maximum sensitivity value is evaluated with respect to the unit length of 1 mm owing to the relatively low-frequency band. However, in the W-band or a higher frequency, it is not suitable to set the unit length of 1 mm, which is a very large value compared with the wavelength. Therefore, the maximum sensitivity is calculated considering $0.1\lambda_0$ as the center frequency. The maximum sensitivity obtained using the proposed method is 2-5 times lower than those of previous low phase sensitivity unit cells.

TABLE 2. Comparison of low phase sensitivity unit cell in previous studies and this work.

	This Work	[10]	[12]		[20]	[21]
Frequency (GHz)	90	15	10	20	10	20
Phase Range (°)	364	360	360		423	360
Element Type	Double	Single	Phoenix (triple)		Double	Multiple
Maximum Phase Sensitivity (°/mm)	310	200	198	148	180	170
Maximum Phase Sensitivity (°/0.1λ_0)	103	400	594	222	540	510

III. WIDEBAND CHARACTERIZATION

A. UNIT CELL CHARACTERISTICS ALONG THE ANGLE OF INCIDENCE

A significant disadvantage of a reflectarray antenna is its narrow bandwidth. To overcome this problem, the bandwidth has been improved through the linearity of the reflection-phase slope at different frequencies [22]–[24]. However, if the design of a unit cell focuses only on the linearity of a phase slope, the phase characteristic could be linear but the phase sensitivity could significantly deteriorate owing to the large slope. In a low-frequency band, even if the sensitivity characteristic is poor, high efficiency can be obtained by considering the manufacturing accuracy of approximately $\pm 10\ \mu$m for a printed circuit board (PCB). However, for high-frequency bands, phase errors may largely occur in typical PCB fabrication processes. Presently, in a W-band or a higher frequency band, the accuracy of a 2-μm silicon-based fabrication process can be used to achieve a large bandwidth and

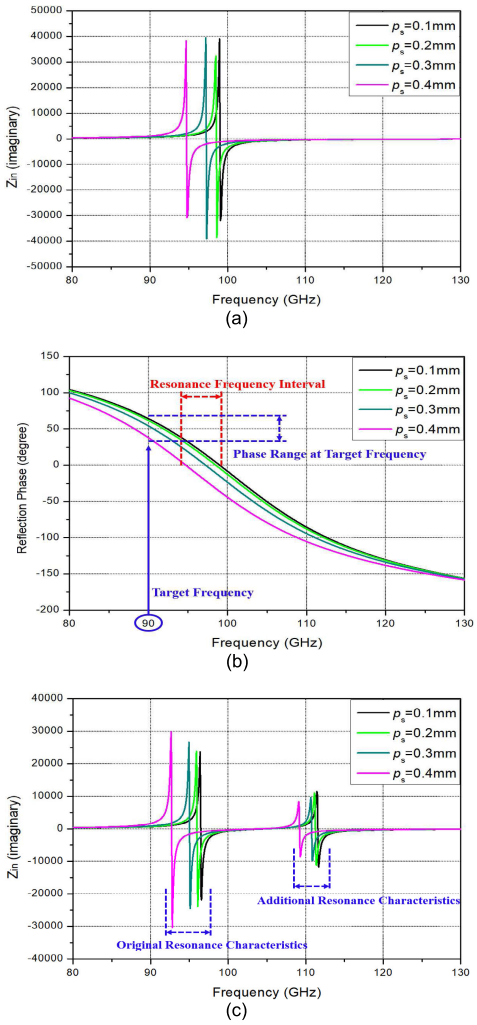

FIGURE 4. Input impedance (imaginary part) and phase range of step 3 of proposed unit cell for $\phi = 90°$. (a) Input impedance of normal incidence ($\theta = 0°$), (b) phase range of normal incidence ($\theta = 0°$), and (c) input impedance of 20° incidence ($\theta = 20°$).

high efficiency despite high phase sensitivity [25]. However, if a typical PCB process is used without using expensive fabrication processes, low phase sensitivity is essential. Low phase sensitivity is favorably accompanied by almost parallel and linear phase slopes of the unit cell because it has a low phase slope rather than the existing S-curve of the reflection phase. However, the reflection phase characteristic for the other frequencies, rather than the center frequency, may vary drastically depending on the angle of incidence. Therefore, it is necessary to confirm the phase characteristics of not only the normal incident angle but also other incident angles by considering the position of the element and the feed horn of the proposed structure. Fig. 4 shows the imaginary part of the input impedance and reflection phase at step 3 of the proposed unit cell depending on the angle of incidence. As shown in Fig. 4 (a), the resonant frequency changes according to the patch size. That is, when the target frequency is near the resonant frequency band, the phase sensitivity

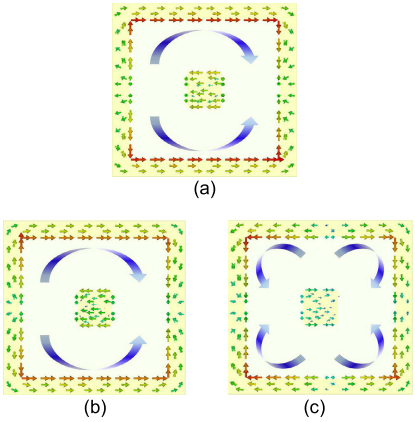

FIGURE 5. Surface current distributions at resonance frequencies according to incident angle for $\phi = 90°$. (a) $f = 97.2$ GHz (normal incidence, $\theta = 0°$), (b) $f = 95.1$ GHz (20° incidence, $\theta = 20°$), (c) $f = 110.4$ GHz (20° incidence, $\theta = 20°$).

of the unit cell depends on the shift rate of the resonant frequency according to the variation in the element length. Fig. 4 (b) shows the reflection phase characteristics of Fig. 4 (a). The shift rate of the resonant frequency is proportional to the phase range at the target frequency near the resonant frequency band. Therefore, in the proposed low phase sensitivity unit cell, the shift interval of the resonant frequency and the phase range at the target frequency are very small, resulting in low phase sensitivity. Thus, the reflection phase at the target frequency can be controlled and derived through the resonance characteristics of the unit cell. Fig. 4 (c) shows the input impedance when the angle of incidence is set to 20°. When the incident angle is varied, an additional resonance owing to the higher-order resonance of conductor elements as well as the original resonance occurring at the normal incidence can be generated. The original resonance occurs from 93 GHz to 98 GHz, and the additional resonance occurs from 109 GHz to 113 GHz. Fig. 5 shows the induced current distribution at the resonance frequencies when the patch size is 0.3 mm. At 20° incidence, the first resonance characteristic is almost the same as that of the normal incidence and resembles the λ loop resonance, indicating that the two resonances are same resonance characteristics. However, the second resonance of 20° incidence occurs as an additional resonance resembling a 2λ loop resonance, which is caused by the higher-order resonance of the conductor elements. In the case of a low-phase sensitivity unit cell, an additional resonant frequency band is likely to occur within a wide target bandwidth, resulting in the serious phase distortion. Therefore, it is necessary to evaluate the deterioration of the phase-frequency characteristics depending on the incidence angle.

B. ARRANGEMENT METHOD OF THE ELEMENTS ON THE ARRAY SURFACE

Fig. 6 shows the reflection phase of the proposed unit cell according to the incident angle at different frequencies for

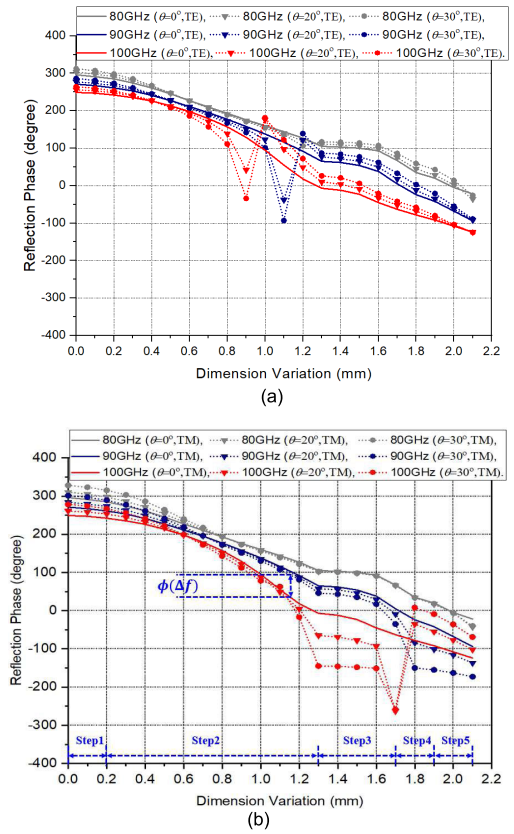

FIGURE 6. Reflection phase range of the proposed unit cell according to the incident angle at different frequencies for $\phi = 90°$. (a) Reflection phase for TE mode, (b) reflection phase for TM mode.

transverse electric (TE) and magnetic (TM) modes. For TE mode, a phase distortion with respect to the incident angle is observed near 1.1 mm and 0.9 mm of dimension variation at 90 GHz and 100 GHz, respectively. In contrast, for TM mode, almost no phase shift with respect to the incident angle is observed at the center frequency of 90 GHz. However, at a high-frequency band, a large–phase deterioration is observed in steps 3–5. At 100 GHz, as the incidence angle increases, the phase shift increases to more than 60°, starting from step 3. As the frequency increases, the phase shift deteriorates more than that of the low-frequency band. To investigate the effect of TE and TM modes on the proposed reflectarray antenna, we calculated the real radiated power for the TE and TM incident waves based on the equivalence principle on the proposed reflectarray surface. The equivalent current sources on reflectarray surface are derived by using full-wave simulation of the pyramidal feed horn. Fig. 7 shows the real radiated power for the TE and TM incident waves. As shown in Fig. 7 (a), which is the normalized radiated power for the TE mode, the radiated power is dominant near the $\phi = 0°$ plane, but not dominant near the $\phi = 90°$ plane. In contrast, Fig. 7 (b), which is the normalized radiated power for the TM mode, also show that the radiated power is dominant near the $\phi = 90°$ plane, but not dominant near the $\phi = 0°$ plane. To analyze the effect of radiated power for

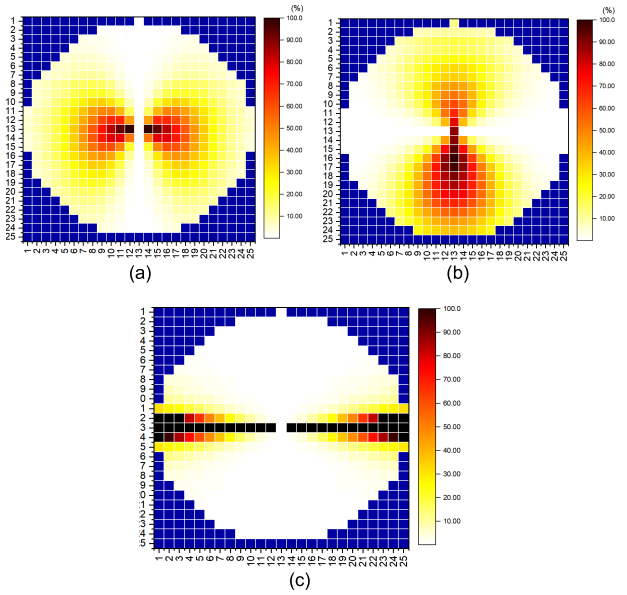

FIGURE 7. Real radiated power on reflectarray elements. (a) Normalized radiated power for TE mode, (b) normalized radiated power for TM mode, (c) ratio of radiated power for TE to that of TM mode.

the TE and TM mode on the proposed reflectarray surface accurately, we calculated the ratio of radiated power for the TE mode to that for the TM mode. Results indicate that in most areas of the reflectarray antenna, the radiated power for the TM mode is very dominant, except near the $\phi = 0°$ plane, as shown Fig. 7 (c). Therefore, to analyze and design the reflectarray antenna effectively, we considered only the reflection phase for TM incident wave in the arrangement method of the proposed reflectarray antenna. Furthermore, the dimension variation of distorted phase with respect to incident angle is wide, as shown in Fig. 6 (b). Therefore, the elements in steps 3–5 should be placed at the appropriate position of the array surface considering the position of the elements and incidence angle of the feed horn. Fig. 8 shows the structure of the proposed reflectarray antenna. An offset structure is selected to reduce the blockage effect of the feeding structure. The offset angle of the structure is 17°, the distance from the phase center of the horn to the center of the array surface is $R_{ref} = 37.6$ mm, and the height of the horn is $h = R_{ref} \cos 17° = 35.95$ mm. The required reflection phase of the element placed on the array surface is calculated as follows [2].

$$\psi_{i,required} = k_0(R_i - \vec{r}_i \cdot \hat{r_0}) + \psi_0 \tag{1}$$

where k_0 is the free-space wavenumber, R_i is the distance between the phase center of the feed horn and the i-th element, $\vec{r}_i$ is the position vector of the i-th element, $\hat{r}_0$ is the unit vector in the main beam direction, and ψ_0 is the constant phase used to determine the initial step number. The relative phase error of an array surface can be calculated with respect to any element in the array [26]. However, as the above-mentioned reference assumes a normal incident angle, the phase characteristics according to the angle of incidence

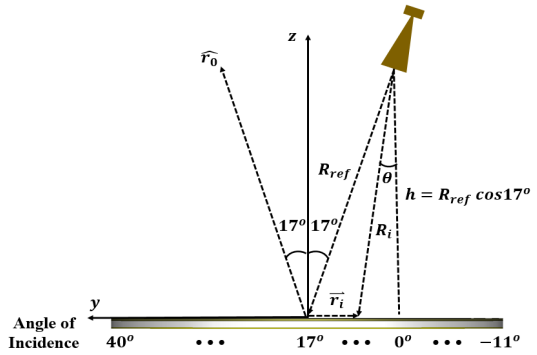

FIGURE 8. 2D-structural dimensions of the proposed reflectarray antenna for $\phi = 90°$.

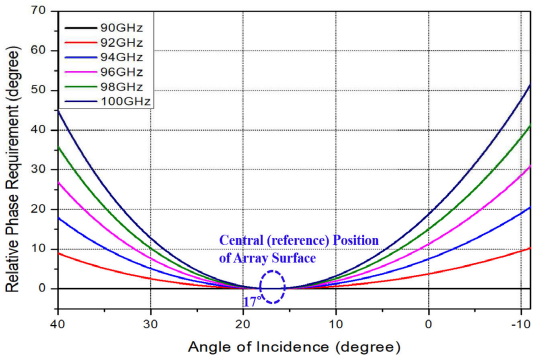

FIGURE 9. Relative phase requirement according to incidence angle for $\phi = 90°$.

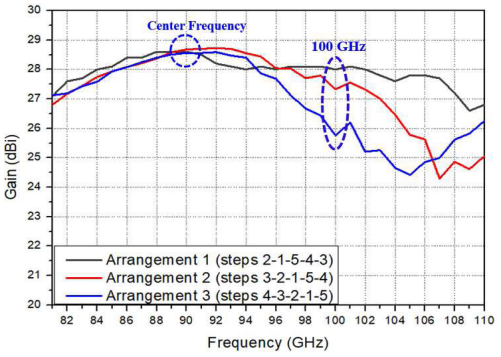

FIGURE 10. Performance of reflectarray antenna at different arrangements of elements on the array surface.

are not considered. Thus, to accurately analyze the phase characteristics, we represent the relative phase relation considering the incident angle θ. At $f = f_0$ (target frequency), the required phase $\psi_{i,required}(f_0)$ is almost equal to the reflection phase $\psi_i(f_0)$ of the element because $\psi_i(f_0)$ is derived by unit cell simulation depending on the normal incident angle. The center of the reflectarray surface is considered as a reference for phase calculation. Thus, the reflection phases of the central and side positions of an array surface are represented by (2) and (3), respectively.

$$\psi_{ref,required}(f_0) = k_0 R_{ref} + \psi_0 \cong \psi_{ref}(f_0) \quad (2)$$

$$\psi_{i,required}(f_0) = k_0(R_i - \vec{r_i} \cdot \hat{r_0}) + \psi_0 \cong \psi_i(f_0) \quad (3)$$

Under this condition, if the frequency changes, the reflection phase relation is distorted. At $f = f_s$, the wave number of the required phase changes from k_0 to k_s, and the phase of the element changes from $\psi_i(f_0)$ to $\psi_i(f_s)$, resulting in phase mismatch with the required phase; this relation is represented as follows.

$$\begin{aligned}\psi_{ref,required}(f_s) &= k_s R_{ref} + \psi_0 \\ &\neq \psi_{ref}(f_s) \cong \psi_{ref}(f_0) + \Delta\psi_{ref}(\Delta f) \quad (4)\\ \psi_{i,required}(f_s) &= k_s\left(R_i - \vec{r_i} \cdot \hat{r_0}\right) + \psi_0 \\ &\neq \psi_i(f_s) \cong \psi_i(f_0) + \Delta\psi_i(\Delta f) \quad (5)\end{aligned}$$

where $\Delta\psi_{ref}(\Delta f)$ and $\Delta\psi_i(\Delta f)$ are the phase shifts of the element at the central and side positions with respect to frequency variation, considering the angle of incidence, respectively. The relative phase error (PE) for the i-th element in the array surface with respect to the central position of the reflectarray is represented as follows, considering the angle of incidence.

$$\begin{aligned}PE_i(f_s) &= \left|\left\{\psi_i(f_s) - \psi_{i,required}(f_s)\right\}\right. \\ &\quad \left. - \left\{\psi_{ref}(f_s) - \psi_{ref,required}(f_s)\right\}\right| \\ &\cong \left|\left\{(k_s - k_0)\left(-R_{ref} + R_i - \vec{r_i} \cdot \hat{r_0}\right)\right\}\right. \\ &\quad \left. + \left\{\Delta\psi_{ref}(\Delta f) - \Delta\psi_i(\Delta f)\right\}\right| \quad (6)\end{aligned}$$

Equation (6) contains two terms: the first term represents the relative phase requirement determined by the frequency and structural dimensions, whereas the second term represents the shifted phase difference $\Delta\psi_{ref}(\Delta f) - \Delta\psi_i(\Delta f)$ of the elements, which are placed in the central and outer positions, with respect to the frequency variation. The proposed unit cell elements exhibit an abrupt phase shift owing to the additional resonance characteristics in certain frequency bands, depending on the incident angle, as described previously. Therefore, the second term should be considered for an abrupt phase shift to compensate for the relative phase requirement Fig. 9 shows the relative phase requirement, which is described by the first term of (6), along the array surface at $\phi = 90°$ represented by the angle of incidence. The relative phase requirement represents the phase relationship between the central and outer positions of the array surface. Therefore, the central position of the array surface, which has an incident angle of 17°, does not have any relative phase requirements at different frequencies, and the relative phase requirement increases from the central to the outer positions of the array surface. To compensate for the relative phase requirement, the shifted phase $\Delta\psi(\Delta f)$ according to frequency variation should be considered based on the angle of incidence. In the normal incidence case, $\Delta\psi(\Delta f)$ is nearly uniform across all dimensions of the unit cell, as shown in Fig. 6 (b). However, in the oblique incidence case, $\Delta\psi(\Delta f)$ is nearly uniform in steps 1 and 2 but increases drastically in steps 3−5. When the dimension of central element of the reflectarray surface is selected to be approximately 1.1 mm, which does not cause

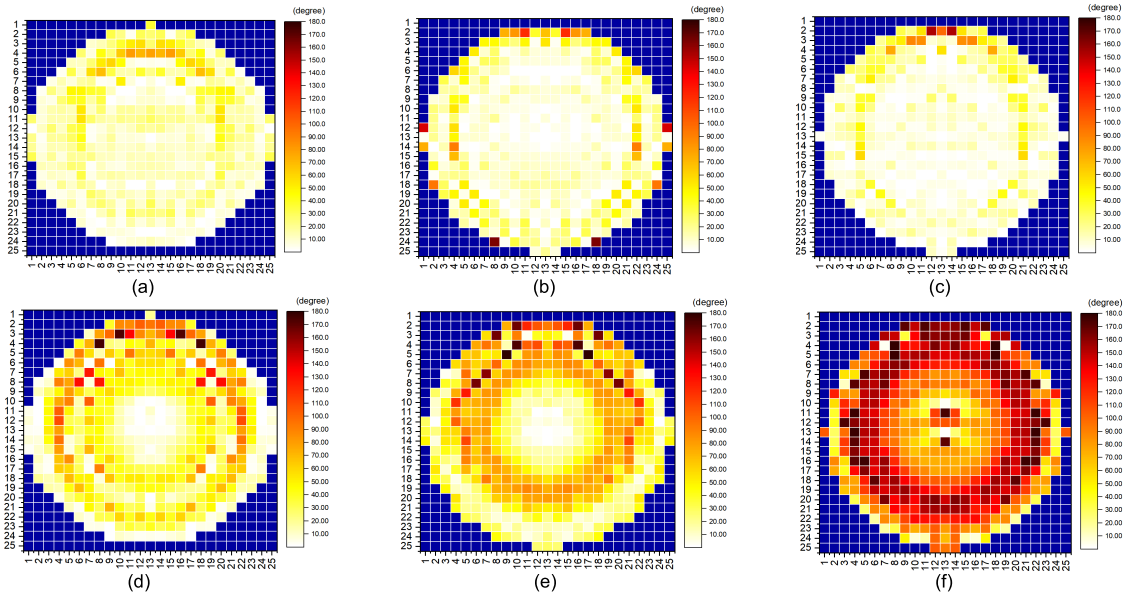

FIGURE 11. Real relative phase error of reflectarray elements at different arrangements. (a) Arrangement 1 at 90 GHz, (b) arrangement 2 at 90 GHz, (c) arrangement 3 at 90 GHz, (d) arrangement 1 at 100 GHz, (e) arrangement 2 at 100 GHz, (f) arrangement 3 at 100 GHz.

phase distortion, $\Delta\psi_{ref}(\Delta f)$ is approximately $-70°$ and $\Delta\psi_i(\Delta f)$ at the outer position gradually increases. Therefore, the shifted phase difference, which is represented by the second term in (6), gradually decreases from the central to the outer position of the array surface, compensating for the relative phase requirement. However, in the outer positions of the array surface, which are comprised of step $5-3$, the phase distortion of the unit cell abruptly increases and does not perfectly satisfy the relative phase requirement. Nevertheless, this step arrangement method can reduce the relative phase error and improve the gain bandwidth because the phase of the outer position of the reflectarray has relatively minimal effect on the antenna performance compared with that of the central position of the reflectarray [27]. Fig. 10 shows the gain performance according to the step arrangements. The order of step arrangement represents the step variation from the central to the outer positions of the array surface. At a center frequency of 90 GHz, the gain performance does not vary considerably. However, as the frequency increases, the gain performance deteriorates according to the arrangements because the phase shift $\Delta\psi_i(\Delta f)$ of arrangements 2 and 3 does not gradually change in the vicinity of the central position of the reflectarray surface. These characteristics indicate that the additional resonance owing to the higher order resonance of resonant elements has severe effect on bandwidth performance rather than the performance at the center frequency. To investigate the correlation between the relative phase error and gain performance, we calculated the real relative phase error of reflectarray elements using full-wave simulation. This calculation method of real phase error is based on the equivalence principle [28]. Fig. 11 shows the real relative phase error of reflectarray elements at different arrangements. As shown in Figs. 11 (a), (b), and (c),

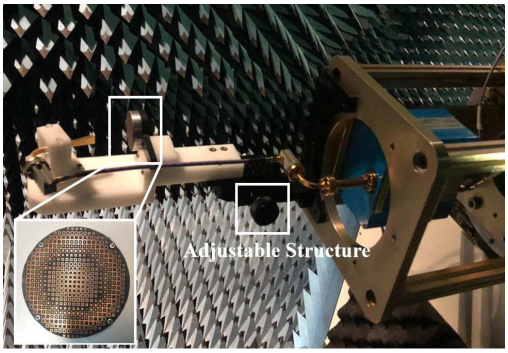

FIGURE 12. Fabricated prototype of reflectarray antenna.

the real relative phase error is generally very low at the center frequency of 90 GHz. It is expected that although there are some elements with the reflection phase distortion for the TE mode at 90 GHz, the effect on the proposed reflectarray surface for the TM mode is very dominant, and the reflection phase for the TM mode at 90 GHz is almost not distorted with respect to the angle of incidence. Moreover, in the arrangement 1, the number of the reflectarray elements consisting of dimension variations of 1 mm to 1.2 mm, which are distorted phase dimensions for the TE mode at 90 GHz, are approximately 13 elements in around $\phi = 90°$ plane. The number of these elements is very small compared to the total number of 448 elements. Hence, these results correlate with the gain performance at 90 GHz at different arrangements. In addition, the real relative phase errors provide different results depending on the arrangement method, as shown in Figs. 11 (d), (e), and (f). In arrangement 1, the real relative phase errors at 100 GHz is somewhat high compared with

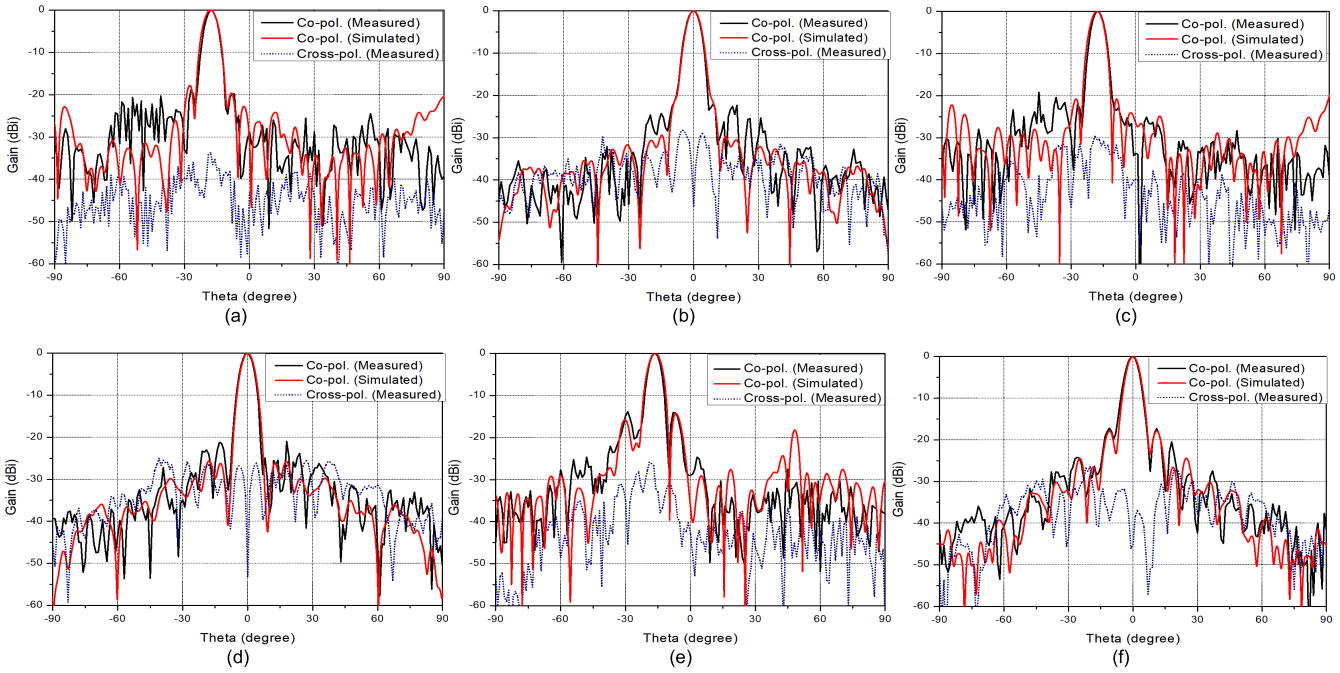

FIGURE 13. Simulated and measured radiation patterns (a) E-plane and (b) H-plane at 85 GHz; (c) E-plane and (d) H-plane at 90 GHz; (e) E-plane and (f) H-plane at 100 GHz.

that at 90 GHz, but generally low compared with different arrangements at 100 GHz. As arrangement increases, the real relative phase errors at 100 GHz are more deteriorated. Thus, in arrangement 3, those are generally very high. These results also correlate with the gain performance at 100 GHz at different arrangements. Therefore, phase distortion along step variation must be considered based on the relative phase requirement. Finally, the arrangement of steps of the final reflectarray antenna is as follows: 2–1–5–4–3.

IV. EXPERIMENTAL RESULTS

In this study, a W-band single-layer reflectarray antenna is designed and fabricated. Fig. 12 shows a prototype of the fabricated antenna, and measurements are conducted in a millimeter-wave non-directional chamber. To connect the source to the offset feed horn, a 90° waveguide and a transition adapter of an RF-cable are used. The strut of the feed horn is fabricated to be able to adjust the antenna position to ensure precise set up of the measurement-jig. A dielectric spacer is used to maintain the air gap. The proposed antenna is designed to have a center frequency of 90 GHz. The aperture diameter is 40 mm and the focal length is 37.6 mm, which satisfies F/D = 0.94. A pyramidal horn is used, and the angle of the main beam is 17°, which is equal to the offset angle. The gain performance was measured using a far-field measurement system with a frequency resolution of 1 GHz. The simulated and measured radiation patterns in the two principal planes, namely E- and H- planes, are shown in Fig. 13 at 85, 90, and 100 GHz for comparison purposes and to observe the performance in the broadband. The figure shows good

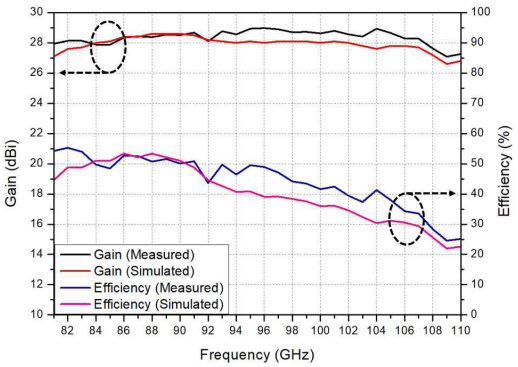

FIGURE 14. Simulated and measured gain and corresponding aperture efficiencies.

agreement between the simulated and measured results. The side-lobe level of the E- and H-planes at the center frequency of 90 GHz are −22 and −21 dB, respectively. The cross-polarization level of E- and H-planes at the center frequency of 90 GHz are −30 and −27 dB, respectively. The maximum side-lobe and cross-polarization level are −14 and −26 dB, respectively. Fig. 14 shows the details of antenna gain and aperture. The slight discrepancy in gain performance of the proposed reflectarray antenna is considered to be caused by the slight discrepancies in the performance of the fabricated and simulated pyramidal horn. The reflectarray antenna performance exhibited a maximum efficiency of 55.3% and 1-dB gain bandwidth of 28.8%, which can be regarded as good performance regarding millimeter waves. Table3 shows the comparison of the obtained results with those of other millimeter

TABLE 3. Comparison of W-band or higher band reflectarray antennas in previous studies and this work.

	This study	[25]	[29]	[30]	[31]
Process	PCB	Silicon	Dielectric	Dielectric	Graphene
Center Frequency (GHz)	90	165	100	220	1300
Aperture size (λ_0)	12	23.7	10	20.5	10.8
1-dB gain bandwidth (%)	28.8	24.2	20.7	20.9	15
Maximum efficiency (%)	55.3	44.7	14.1	27.6	42.58
Measured (Y/N)	Y	Y	Y	Y	N

wave antennas for W-band or higher bands. Compared with conventional antennas, the proposed antenna achieves good performance in terms of efficiency and bandwidth.

V. CONCLUSION

In this study, a W-band reflectarray antenna with low phase sensitivity and wideband characteristics is designed and fabricated, and its performance is verified. The unit cell design approach proposed in this study can achieve a low phase sensitivity performance in a high-frequency band. The reflection phase characteristics of the proposed unit cell are analyzed taking the incidence angle into consideration, and the wideband characteristics are obtained through efficient arrangement of elements on the reflectarray surface. The fabricated reflectarray antenna can achieve a maximum efficiency of 55.3% and 1-dB gain bandwidth of 28.8%.

REFERENCES

[1] D. M. Pozar, S. D. Targonski, and H. D. Syrigos, "Design of millimeter wave microstrip reflectarrays," *IEEE Trans. Antennas Propag.*, vol. 45, no. 2, pp. 287–296, Feb. 1997.

[2] J. Huang and J. A. Encinar, *Reflectarray Antennas*. Piscataway, NJ, USA: IEEE Press, 2008.

[3] J. Huang and R. J. Pogorzelski, "Microstrip reflectarray with elements having variable rotation angles," in *IEEE Antennas Propag. Soc. Int. Symp. Dig.*, vol. 2, Jul. 1997, pp. 1280–1283.

[4] C. R. Dietlein, A. S. Hedden, and D. A. Wikner, "Digital reflectarray considerations for terrestrial millimeter-wave imaging," *IEEE Antennas Wireless Propag. Lett.*, vol. 11, pp. 272–275, 2012.

[5] P. Zheng, B. Hu, S. Xu, and H. Sun, "A W-band high-aperture-efficiency multipolarized monopulse cassegrain antenna fed by phased microstrip patch quad," *IEEE Antennas Wireless Propag. Lett.*, vol. 16, pp. 1609–1613, 2017.

[6] B. Mencia-Oliva, J. Grajal, O. A. Yeste-Ojeda, G. Rubio-Cidre, and A. Badolato, "Low-cost CW-LFM radar sensor at 100 GHz," *IEEE Trans. Microw. Theory Techn.*, vol. 61, no. 2, pp. 986–998, Feb. 2013.

[7] S. R. Lee, E. H. Lim, F. L. Lo, and W. H. Ng, "Circularly polarized elliptical microstrip patch reflectarray," *IEEE Trans. Antennas Propag.*, vol. 65, no. 8, pp. 4322–4327, Aug. 2017.

[8] M. Bozzi, S. Germani, and L. Perregrini, "Performance comparison of different element shapes used in printed reflectarrays," *IEEE Antennas Wireless Propag. Lett.*, vol. 2, pp. 219–222, 2003.

[9] K. H. Sayidmarie and M. E. Bialkowski, "Fractal unit cells of increased phasing range and low slopes for single-layer microstrip reflectarrays," *IET Microw., Antennas Propag.*, vol. 5, no. 11, pp. 1371–1379, 2011.

[10] J. H. Yoon, Y. J. Yoon, W.-S. Lee, and J.-H. So, "Square ring element reflectarrays with improved radiation characteristics by reducing reflection phase sensitivity," *IEEE Trans. Antennas Propag.*, vol. 63, no. 2, pp. 814–818, Feb. 2015.

[11] J. Ethier and M. R. J. C. Shaker, "Reflectarray design comprised of sub-wavelength coupled-resonant square loop elements," *Electron. Lett.*, vol. 47, no. 22, pp. 1215–1217, 2011.

[12] R. Deng, S. Xu, F. Yang, and M. Li, "Single-layer dual-band reflectarray antennas with wide frequency ratios and high aperture efficiencies using phoenix elements," *IEEE Trans. Antennas Propag.*, vol. 65, no. 2, pp. 612–622, Feb. 2017.

[13] A. Vosoogh, K. Keyghobad, A. Khaleghi, and S. Mansouri, "A high-efficiency Ku-band reflectarray antenna using single-layer multiresonance elements," *IEEE Antennas Wireless Propag. Lett.*, vol. 13, pp. 891–894, 2014.

[14] J. A. Encinar, "Design of two-layer printed reflectarrays using patches of variable size," *IEEE Trans. Antennas Propag.*, vol. 49, no. 10, pp. 1403–1410, Oct. 2001.

[15] C. S. Geaney, M. Hosseini, and S. V. Hum, "Reflectarray antennas for independent dual linear and circular polarization control," *IEEE Trans. Antennas Propag.*, vol. 67, no. 9, pp. 5908–5918, Sep. 2019.

[16] P. Nayeri, F. Yang, and A. Z. Elsherbeni, "A broadband microstrip reflectarray using sub-wavelength patch elements," in *Proc. IEEE Antennas Propag. Soc. Int. Symp.*, Jun. 2009, pp. 1–4.

[17] M. Min and L. Guo, "Design of a wideband single-layer reflectarray antenna using slotted rectangular patch with concave arms," *IEEE Access*, vol. 7, pp. 176197–176203, 2019.

[18] K. Mayumi, H. Deguchi, and M. Tsuji, "Wideband single-layer microstrip reflectarray based on multiple-resonance behavior," in *Proc. IEEE Antennas Propag. Soc. Int. Symp.*, Jul. 2008, pp. 1–4.

[19] R. Deng, S. Xu, F. Yang, and M. Li, "A single-layer high-efficiency wideband reflectarray using hybrid design approach," *IEEE Antennas Wireless Propag. Lett.*, vol. 16, pp. 884–887, 2017.

[20] B. Mohammadi, J. Nourinia, C. Ghobadi, A. Mahmoud, M. Karamirad, F. Alizadeh, and H. Mardani, "Enhanced reflectarray antenna using elements with reduced reflection phase sensitivity," *IEEE Antennas Wireless Propag. Lett.*, vol. 17, no. 7, pp. 1334–1338, Jul. 2018.

[21] T. Cai, G.-M. Wang, and X.-F. Zhang, "Compact dual-resonance element with low phase sensitivity for offset reflectarray antennas," *IEEE Antennas Wireless Propag. Lett.*, vol. 16, pp. 1213–1216, 2017.

[22] M. R. Chaharmir and J. Shaker, "Broadband reflectarray with combination of cross and rectangle loop elements," *Electron. Lett.*, vol. 44, no. 11, pp. 658–659, May 2008.

[23] X. Xia, Q. Wu, H. Wang, C. Yu, and W. Hong, "Wideband millimeter-wave microstrip reflectarray using dual-resonance unit cells," *IEEE Antennas Wireless Propag. Lett.*, vol. 16, pp. 4–7, 2007.

[24] F. Xue, H.-J. Wang, M. Yi, G. Liu, and X.-C. Dong, "Design of a broadband single-layer linearly polarized reflectarray using four-arm spiral elements," *IEEE Antennas Wireless Propag. Lett.*, vol. 16, pp. 696–699, 2017.

[25] Z.-W. Miao, Z.-C. Hao, and Q. Yuan, "Design and implementation of a G-band silicon-based single-layer reflectarray antenna," *IEEE Antennas Wireless Propag. Lett.*, vol. 16, pp. 2191–2194, 2017.

[26] P. Nayeri, F. Yang, and A. Z. Elsherbeni, "Broadband reflectarray antennas using double-layer subwavelength patch elements," *IEEE Antennas Wireless Propag. Lett.*, vol. 9, pp. 1139–1142, 2010.

[27] C. Tienda, J. A. Encinar, M. Arrebola, M. Barba, and E. Carrasco, "Design, manufacturing and test of a dual-reflectarray antenna with improved bandwidth and reduced cross-polarization," *IEEE Trans. Antennas Propag.*, vol. 61, no. 3, pp. 1180–1190, Mar. 2013.

[28] E.-C. Choi and S. Nam, "Analysis and elimination of unwanted resonances for wideband reflectarray antenna design," *IEEE Trans. Antennas Propag.*, to be published.

[29] P. Nayeri, M. Liang, R. A. Sabory-Garcia, M. Tuo, F. Yang, M. Gehm, H. Xin, and A. Z. Elsherbeni, "3D printed dielectric reflectarrays: Low-cost high-gain antennas at sub-millimeter waves," *IEEE Trans. Antennas Propag.*, vol. 62, no. 4, pp. 2000–2008, Apr. 2014.

[30] M. D. Wu, B. Li, Y. Zhou, D. L. Guo, Y. Liu, F. Wei, and X. Lv, "Design and measurement of a 220 GHz wideband 3-D printed dielectric reflectarray," *IEEE Antennas Wireless Propag. Lett.*, vol. 17, no. 11, pp. 2094–2098, Nov. 2018.

[31] E. Carrasco and J. Perruisseau-Carrier, "Reflectarray antenna at terahertz using graphene," *IEEE Antennas Wireless Propag. Lett.*, vol. 12, pp. 253–256, 2013.

EUN-CHEOL CHOI received the B.S. and M.S. degrees in electronics, telecommunications and computer engineering from Korea Aerospace University, Goyang, in 2012 and 2014, respectively. He is currently pursuing the Ph.D. degree with Seoul National University, Seoul, South Korea.

His research interests include microwave and millimeter-wave, and reflectarray antenna design and analysis.

SANGWOOK NAM (Senior Member, IEEE) received the B.S. degree from Seoul National University, Seoul, South Korea, in 1981, the M.S. degree from the Korea Advanced Institute of Science and Technology (KAIST), Seoul, in 1983, and the Ph.D. degree from The University of Texas at Austin, Austin, TX, USA, in 1989, all in electrical engineering. From 1983 to 1986, he was a Researcher with the Gold Star Central Research Laboratory, Seoul. Since 1990, he has been a Professor with the School of Electrical Engineering and Computer Science, Seoul National University. His research interests include analysis/design of electromagnetic (EM) structures, antennas, and microwave active/passive circuits.